Iterative Phase Retrieval

James R. Fienup

Veridian Systems
P.O. Box 134008, Ann Arbor, MI 48113-4008
jim.fienup@veridian.com

17 May, 2001

Presented to the Workshop on New Approaches to the
Phase Problem for Non-Periodic Objects,
Lawrence Berkeley National Laboratory

Abstract and References

Abstract
Over 25 years of phase retrieval are reviewed. Application areas include astronomy,[1,2] space-object imaging with both passive-incoherent[3] and active-coherent[4,5,6,7] illumination, wave-front and telescope-misalignment sensing,[8,9,10,11,12,13] 3-D coherent imaging,[14] and synthetic-aperture radar.[15,16,17] Algorithmic approaches include modifications of the Gerchberg-Saxton algorithm[18] such as the hybrid input-output algorithm,[1,19] gradient-search error-minimization techniques,[9,19] approaches to climbing out of stagnation, [20] support estimation from autocorrelation support,[21,22] phase diversity,[12,13] and sharpness maximization algorithms.[17]

References

1. J.R. Fienup, "Reconstruction of an Object from the Modulus of Its Fourier Transform," Opt. Lett. 3, 27-29 (l978).

2. J.C. Dainty and J.R. Fienup, "Phase Retrieval and Image Reconstruction for Astronomy," Chapter 7 in H. Stark, ed., Image Recovery: Theory and Application (Academic Press, 1987), pp. 231-275.

3. J.R. Fienup, "Space Object Imaging Through the Turbulent Atmosphere," Opt. Eng. l8, 529-534 (l979).

4. J.R. Fienup, "Reconstruction of a Complex-Valued Object from the Modulus of Its Fourier Transform Using a Support Constraint," J. Opt. Soc. Am. A 4, 118-123 (1987).

5. P.S. Idell, J.R. Fienup and R.S. Goodman, "Image Synthesis from Nonimaged Laser Speckle Pattems," Opt. Lett. 12, 858-860 (1987).

6. J.R. Fienup and A.M. Kowalczyk, "Phase Retrieval for a Complex-Valued Object by Using a Low-Resolution Image," J. Opt. Soc. Am. A 7, 450-458 (1990).

7. J.N. Cederquist, J.R. Fienup, J.C. Marron and R.G. Paxman, "Phase Retrieval from Experimental Far-Field Data," Opt. Lett. 13, 619-621 (1988).

8. J.N. Cederquist, J.R. Fienup, C.C. Wackerman, S.R. Robinson and D. Kryskowski, "Wave-Front Phase Estimation from Fourier Intensity Measurements," J. Opt. Soc. Am. A 6, 1020-1026 (1989).

9. J.R. Fienup, "Phase-Retrieval Algorithms for a Complicated Optical System," Appl. Opt. 32, 1737-1746 (1993).

10. J.R. Fienup, J.C. Marron, T.J. Schulz and J.H. Seldin, "Hubble Space Telescope Characterized by Using Phase Retrieval Algorithms," Appl. Opt. 32 1747-1768 (1993).

References (cont'd)

11. J.R. Fienup, "Phase Retrieval for Undersampled Broadband Images," J. Opt. Soc. Am. A, 16, 1831-1839 (July 1999).

12. R.G. Paxman and J.R. Fienup, "Optical Misalignment Sensing and Image Reconstruction Using Phase Diversity," J. Opt. Soc. Am. A 5, 914-923 (1988).

13. R.G. Paxman, T.J. Schulz and J.R. Fienup, "Joint Estimation of Object and Aberrations Using Phase Diversity," J. Opt. Soc. Am. A 9, 1072-85 (1992).

14. J.R. Fienup, R.G. Paxman, M.F. Reiley, and B.J. Thelen, "3-D Imaging Correlography and Coherent Image Reconstruction," in Proc. SPIE 3815-07, Digital Image Recovery and Synthesis IV, July 1999, Denver, CO., pp. 60-69.

15. S.A. Werness, M.A. Stuff and J.R. Fienup, "Two Dimensional Imaging of Moving Targets in SAR Data," in 24th Asilomar Conference on Signals, Systems and Computating, paper MP5, November 1990.

16. J.R. Fienup, "Gradient-Search Phase Retrieval Algorithm for Inverse Synthetic Aperture Radar," Optical Engineering 33, 3237-3242 (1994).

17. J.R. Fienup, "Synthetic-Aperture Radar Autofocus by Maximizing Sharpness," Optics Letters 25, 221-223 (15 February 2000).

18. J.R. Fienup, "Iterative Method Applied to Image Reconstruction and to Computer-Generated Holograms," Opt. Eng. l9, 297-305 (l980).

19. J.R. Fienup, "Phase Retrieval Algorithms: A Comparison," Appl. Opt. 2l, 2758-2769 (1982).

20. J.R. Fienup and C.C. Wackerman, "Phase Retrieval Stagnation Problems and Solutions," J. Opt. Soc. Am. A 3, 1897-1907 (1986).

21. J.R. Fienup, T.R. Crimmins, and W. Holsztynski, "Reconstruction of the Support of an Object from the Support of Its Autocorrelation," J. Opt. Soc. Am. 72, 6l0-624 (l982).

22. T.R. Crimmins, J.R. Fienup and B.J. Thelen, "Improved Bounds on Object Support from Autocorrelation Support and Application to Phase Retrieval," J. Opt. Soc. Am. A 7, 3-13 (1990).

Outline

- Examples of Phase Retrieval Applications
- Phase Retrieval Basics
  - Definition
  - Constraints
- Iterative-Transform Phase Retrieval Algorithms
  - Error-Reduction
  - Hybrid Input-Output
  - Gradient Search Nonlinear Optimization
- Wavefront Sensing for Broadband, Undersampled Data
- Support Reconstruction
- 3-D Reconstruction of Coherently Illuminated Opaque Objects
  - Imaging Correlography
  - Laboratory Demonstration
- Phase Diversity
- SAR Autofocus

Passive Imaging of Space Objects

- Problem: atmospheric turbulence limits resolution to

  ≈ 1 arc-sec $\approx 5*10^{-6}$rad. $\approx \dfrac{\lambda}{r_o}$ for $\lambda = 0.5$ microns and $r_o = 10$ cm

  — as compared with Keck 10 m telescope diffraction limit of

  $\dfrac{\lambda}{D} = 0.01$ arc-sec $= 0.05*10^{-6}$rad.

  — 100x factor of improvement possible !

- Solutions:

  — Hubble Space Telecope (2.4 m diam.), \$2 B

  — Adaptive optics + laser guide star, \$10's M

  — Optical interferometry, \$10's M

  — Stellar speckle interferometry, < \$1 M

Labeyrie's Stellar Speckle Interferometry

1. Record blurred images: $g_k(x, y) = f(x, y) * s_k(x, y)$, $k = 1, \ldots, K$

   where $s_k(x, y)$ is k^{th} point-spread function due to atmospheric tubulence

2. Fourier transform: $G_k(u, v) = F(u, v)\, S_k(u, v)$, $k = 1, \ldots, K$

   where $S_k(u, v)$ is k^{th} optical transfer function

3. Magnitude square and average: $\frac{1}{K}\sum_{k=1}^{K} |G_k(u, v)|^2 = |F(u, v)|^2 \frac{1}{K}\sum_{k=1}^{K} |S_k(u, v)|^2$

4. Measure or determine transfer function $\frac{1}{K}\sum_{k=1}^{K} |S_k(u, v)|^2$

   — atmospheric model or measure reference star

5. Divide by $\frac{1}{K}\sum_{k=1}^{K} |S_k(u, v)|^2$ to obtain $|F(u, v)|^2$

Reference: A. Labeyrie, "Attainment of Diffraction Limited Resolution in Large Telescopes by Fourier Analysing Speckle Patterns in Star Images," Astron. and Astrophys. 6, 85-87 (l970).

Phase Retrieval Basics

Fourier transform: $F(u, v) = \iint_{-\infty}^{\infty} f(x, y)\, e^{-i2\pi(ux + vy)}\, dx\, dy$

$$= |F(u, v)|\, e^{i\psi(u, v)} = \mathcal{F}[f(x, y)]$$

Inverse transform: $f(x, y) = \iint_{-\infty}^{\infty} F(u, v)\, e^{+i2\pi(ux + vy)}\, dx\, dy = \mathcal{F}^{-1}[F(u, v)]$

Phase retrieval problem:

> Given $|F(u, v)|$ and some constraints on $f(x, y)$,
>
> Reconstruct $f(x, y)$ or, equivalently, retrieve the phase $\psi(u, v)$

Inherent ambiguities:

$$|F(u, v)| = |\mathcal{F}[f(x, y)]| = |\mathcal{F}[e^{ic} f(x - x_o, y - y_o)]| = |\mathcal{F}[e^{ic} f^*(-x - x_o, -y - y_o)]|$$

(phase constant, images shifts, twin image all result in same data)

Autocorrelation:

$$r_f(x, y) = \iint_{-\infty}^{\infty} f(x', y')\, f^*(x' - x, y' - y)\, dx'\, dy' = \mathcal{F}^{-1}[|F(u, v)|^2]$$

Nonnegativity and Support Constraints

- Nonnegativity constraint: $f(x, y) \geq 0$
  - True for ordinary incoherent imaging, crystallography, MRI, etc.
  - Not for coherent imaging, e.g., SAR, ultrasound imaging, HLR

- The support of an object is the set of points over which it is nonzero
- This is meaningful for objects on dark backgrounds
  - E.g., satellites, astronomical objects, missiles, laser-illuminated objects
  - Or may have known support, such as for retrieving the aberrations of HST
- When imaging phase is totally destroyed,
  a support constraint is essential for image reconstruction
- When an image is formed with some residual phase errors,
  a support constraint can be used to correct the residual errors
  and improve image quality

Optimization Techniques

Minimize error metric by

- ✓ Iterative transform algorithm (Gerchberg-Saxton/Fienup)
- ✓ Gradient search (steepest descent, conjugate gradient, . . .)
- Cut & try
- Damped least squares (Newton-Raphson)
- Linear programming
- Neural network
- etc.

Iterative Transform Algorithm

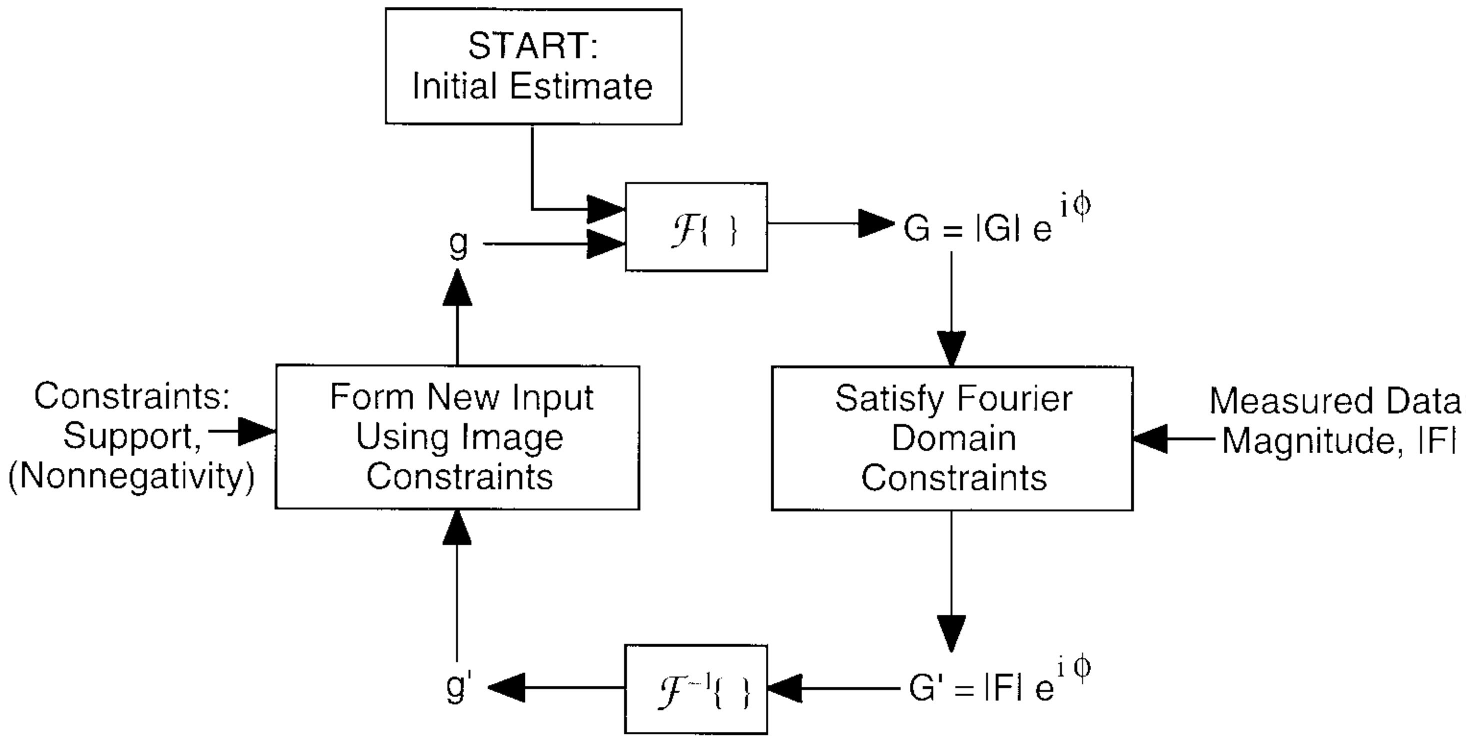

VERIDIAN
ERIM International

Error Reduction = Projection onto Sets

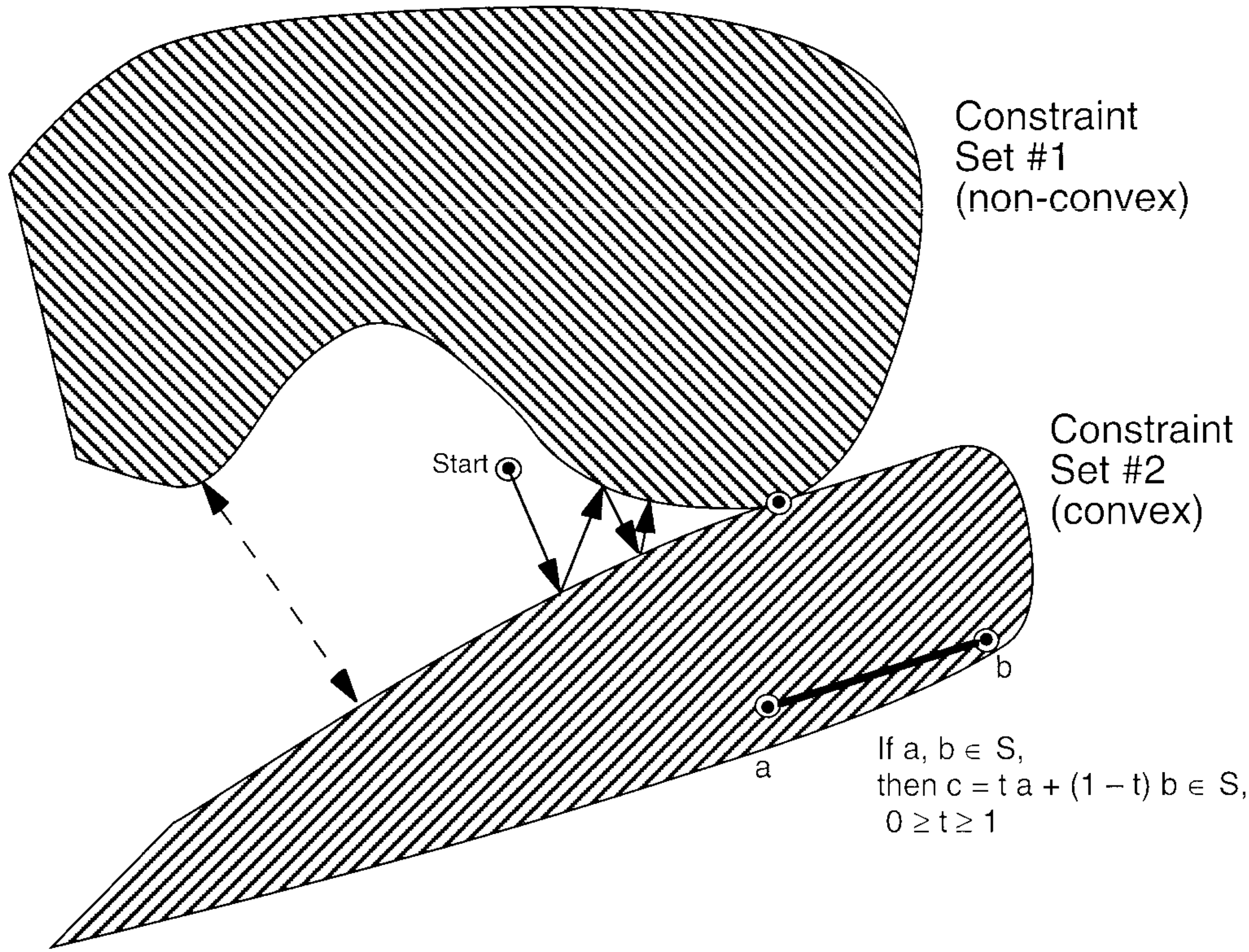

Error Reduction Algorithm versus Gradient Search

Minimize $E_{F,k} = \sum_u [|G_k(u)| - |F(u)|]^2$, where $G_k(u) = \sum_x g_k(x)\, e^{-i2\pi u \bullet x/N}$

constrained by $g_k(x) \geq 0\ ,\ \ \forall x$

Steepest descent gradient search: $g_{k+1}(x) = g_k(x) + \text{step} \bullet \left(-\dfrac{\partial E_{F,k}}{\partial g(x)} \right)$

where $\dfrac{\partial E_{F,k}}{\partial g(x)} = 2 \sum_u [|G_k(u)| - |F(u)|] \dfrac{\partial |G_k(u)|}{\partial g(x)} = 2\, N^2\, [g_k(x) - g_k'(x)]$

and $\mathcal{F}[g_k'(x)] = G_k'(u) = |F(u)| \dfrac{G_k(u)}{|G_k(u)|}$

Linear approximation to E_F yields step size such that

$$g_{k+1}(x) = g_k(x) + (1/2)[g_k'(x) - g_k(x)]$$

or, since E_F is quadratic, use double step size:

$$g_{k+1}(x) = g_k(x) + [g_k'(x) - g_k(x)] = g_k'(x)$$

That is, steepest descent does same thing as error-reduction algorithm

Error-Reduction Algorithm

Error-reduction algorithm can be viewed as

- Projection onto (nonconvex) sets
- Steepest descent gradient search algorithms
- Successive approximations

Error-reduction algorithm has convergence proof:

$$E_F(\text{iter. } n+1) \le E_o(\text{iter. } n) \le E_F(\text{iter. } n)$$

where
$$E_F = \left[\frac{\sum_{uv} [|G(u,v)| - |F(u,v)|]^2}{\sum_{uv} |F(u,v)|^2} \right]^{1/2}, \qquad E_o = \left[\frac{\sum_{xy \notin OK} |g'(x,y)|^2}{\sum_{xy} |g'(x,y)|^2} \right]^{1/2}$$

Hybrid input-output algorithm

— No convergence proof — error metric may even increase

— In practice converges much faster

Iterative Transform Algorithm Variants

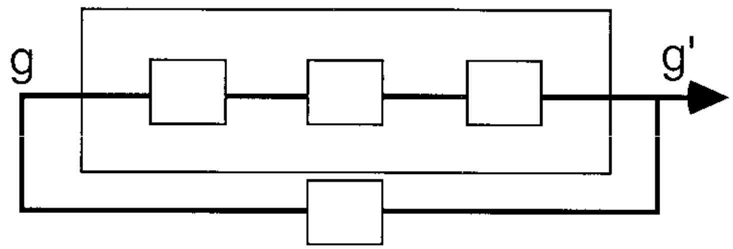

Error reduction

$$g_{k+1} = \begin{cases} g'_k \ , & mn \in OK \\ 0 \ , & mn \in notOK \end{cases}$$

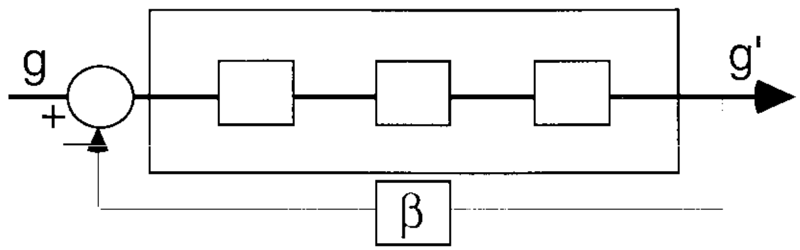

Basic input-output

$$g_{k+1} = \begin{cases} g_k \ , & mn \in OK \\ g_k - \beta g'_k \ , & mn \in notOK \end{cases}$$

Output-output

$$g_{k+1} = \begin{cases} g'_k \ , & mn \in OK \\ g'_k - \beta g'_k \ , & mn \in notOK \end{cases}$$

Hybrid input-output

$$g_{k+1} = \begin{cases} g'_k \ , & mn \in OK \\ g_k - \beta g'_k \ , & mn \in notOK \end{cases}$$

First Phase Retrieval Result

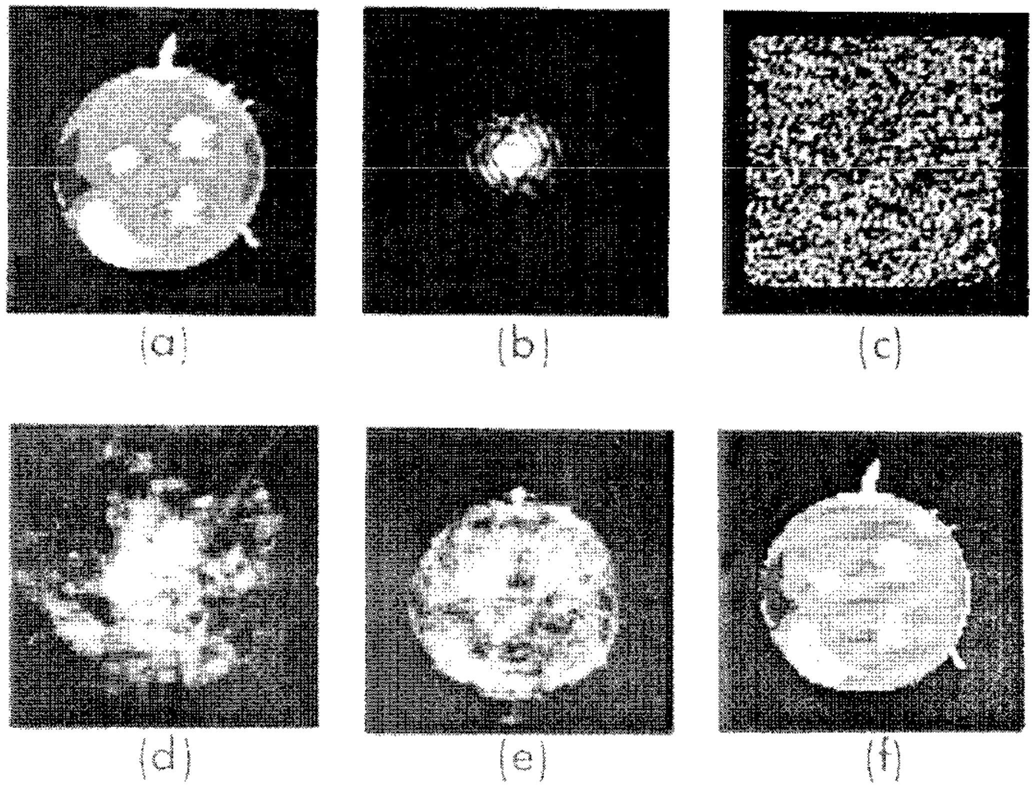

(a) Original object, (b) Fourier modulus data, (c) Initial estimate
(d) – (f) Reconstructed images — number of iterations: (d) 20, (e) 230, (f) 600

Reference: J.R. Fienup, Optics Letters, Vol 3., pp. 27-29 (1978).

Image Reconstruction from Simulated Speckle Interferometry Data

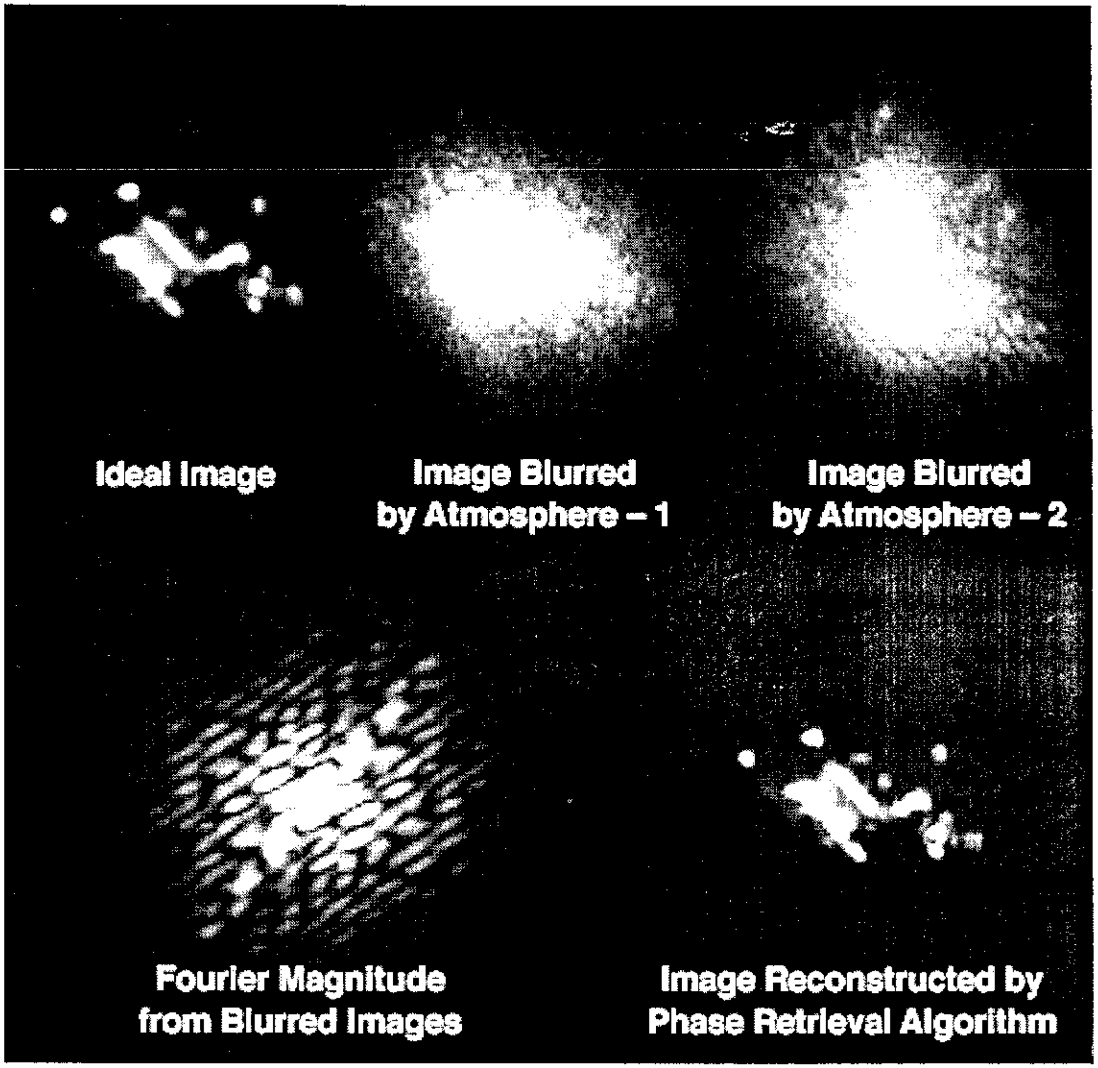

Error Metric versus Iteration Number

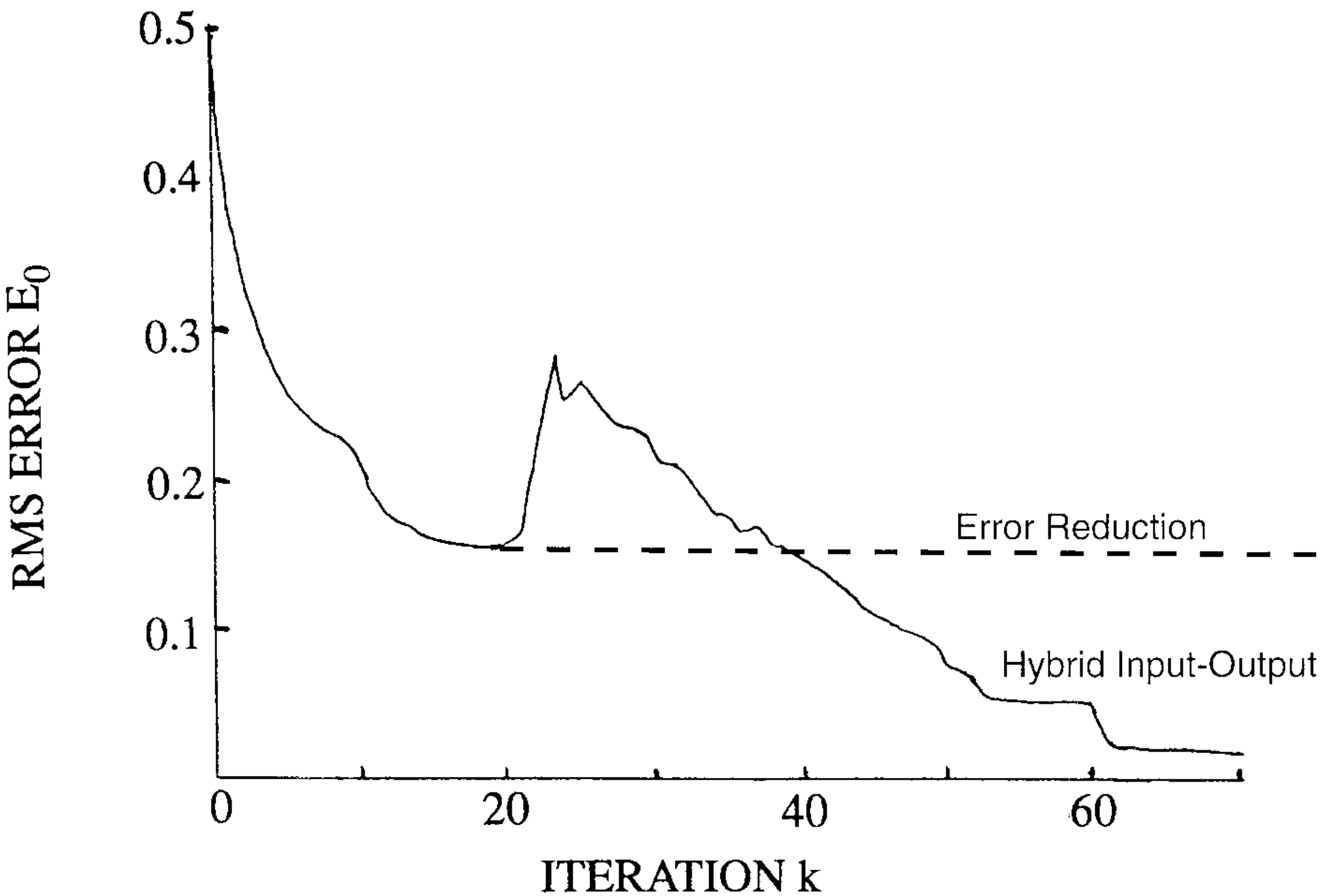

Object and Autocorrelation Supports

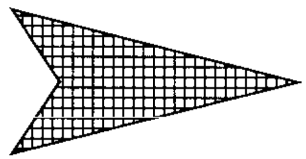

Object
Support

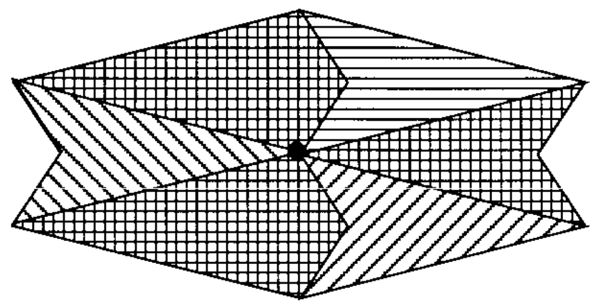

Forming Autocorrelation Support

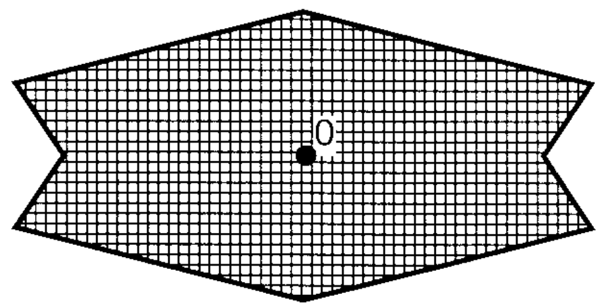

Autocorrelation Support

Bounds on Object Support

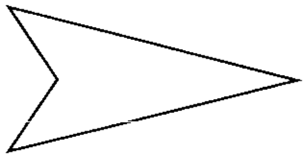

Object
Support

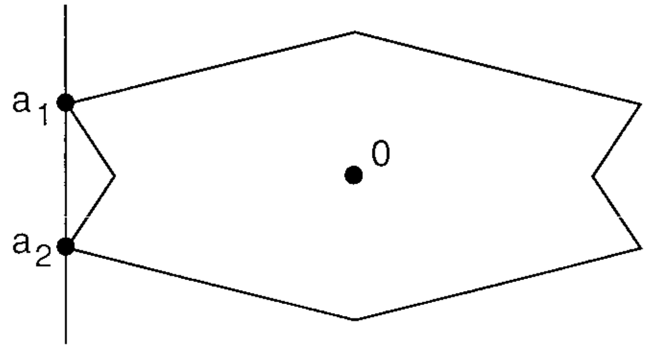

Autocorrelation Support

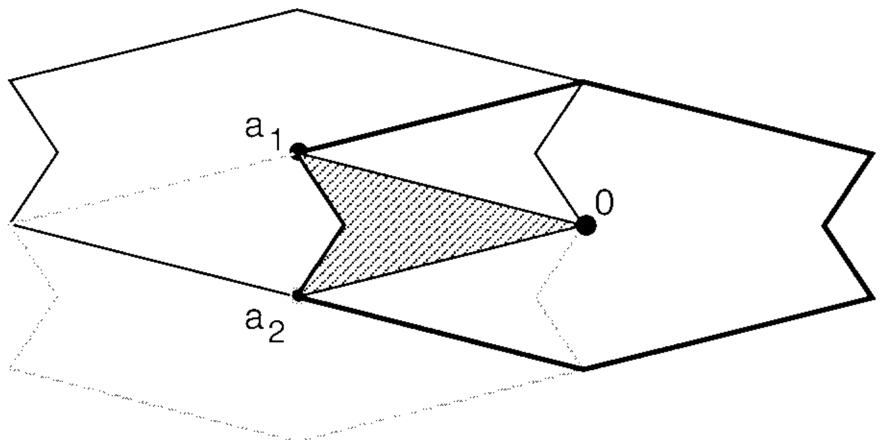

Triple Intersection of Autocorrelation Supports

- Triple-Intersection Rule [Crimmins, Fienup, & Thelen, JOSA A **7**, 3 (1990)]

Triple Intersection for Triangle Object

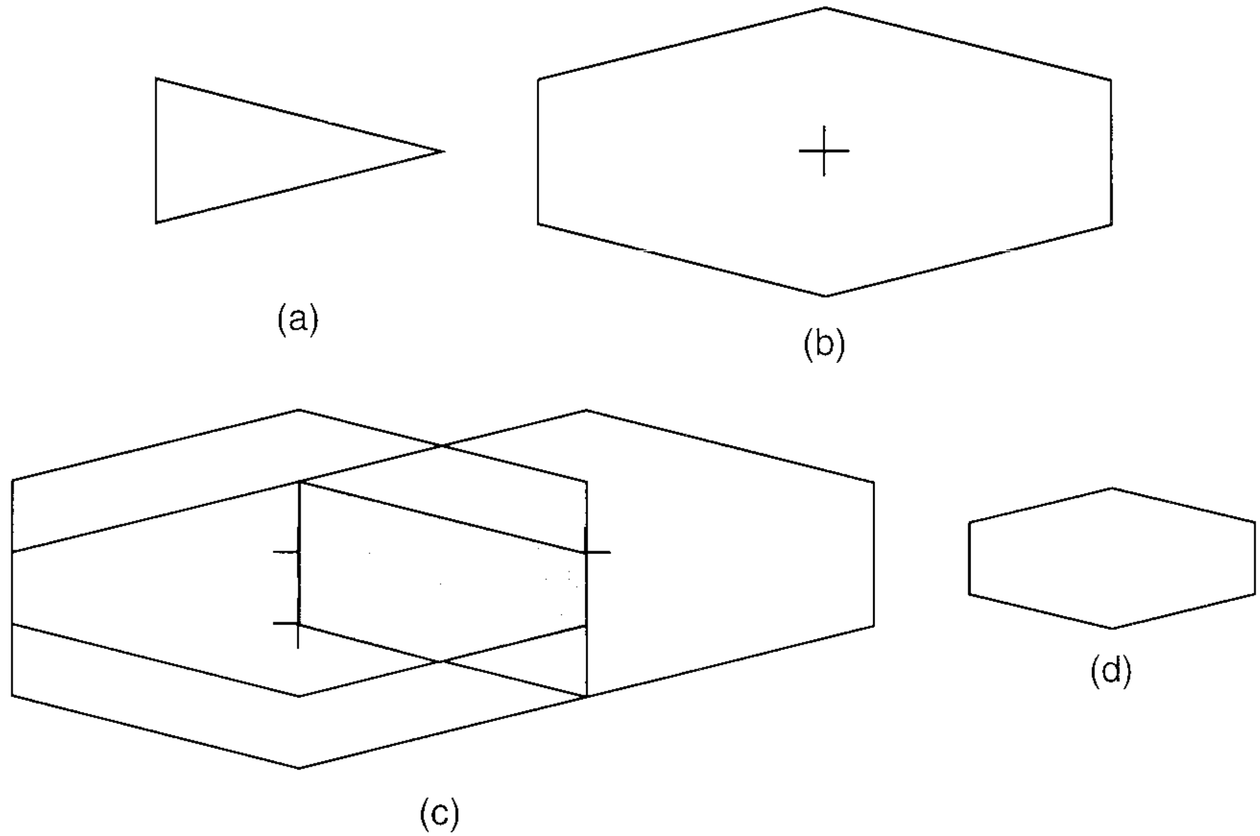

- Family of solutions for object support from autocorrelation support
- Use upper bound for support constraint in phase retrieval
- Does not imply ambiguity of phase retrieval per se

Overcoming Striping Stagnation

- HIO can climb out of many local minima
  - J.H. Seldin and J.R. Fienup, "Numerical Investigation of the Uniqueness of Phase Retrieval," J. Opt. Soc. Am. A 7, 412-427 (1990).
  - H. Takajo, T. Takahashi *et al.*, "Study on the convergence property of the hybrid input output algorithm used for phase retrieval," J. Opt. Soc. Am. A 15, 2849 (1997).
  - H. Takajo, T. Takahashi, T. Shizuma, "Further study on the convergence property of the hybrid inputoutput algorithm used for phase retrieval," J.Opt.Soc. Am. A 16, 2163 (1998)

- Robust local minima often associated with Fourier zeros
  - Whether the Fourier transform has a zero or just a near-zero
    - With noise and sampling, it is not obvious
  - At zeros: phase branch cuts = knots = vortices = screw dislocations
  - Causes striping artifact in real, nonnegative imagery
  - Can be overcome by voting or patching algorithms
    - J.R. Fienup and C.C. Wackerman, "Phase Retrieval Stagnation Problems and Solutions," J. Opt. Soc. Am. A 3, 1897-1907 (1986).

Determine HST Aberrations from PSF

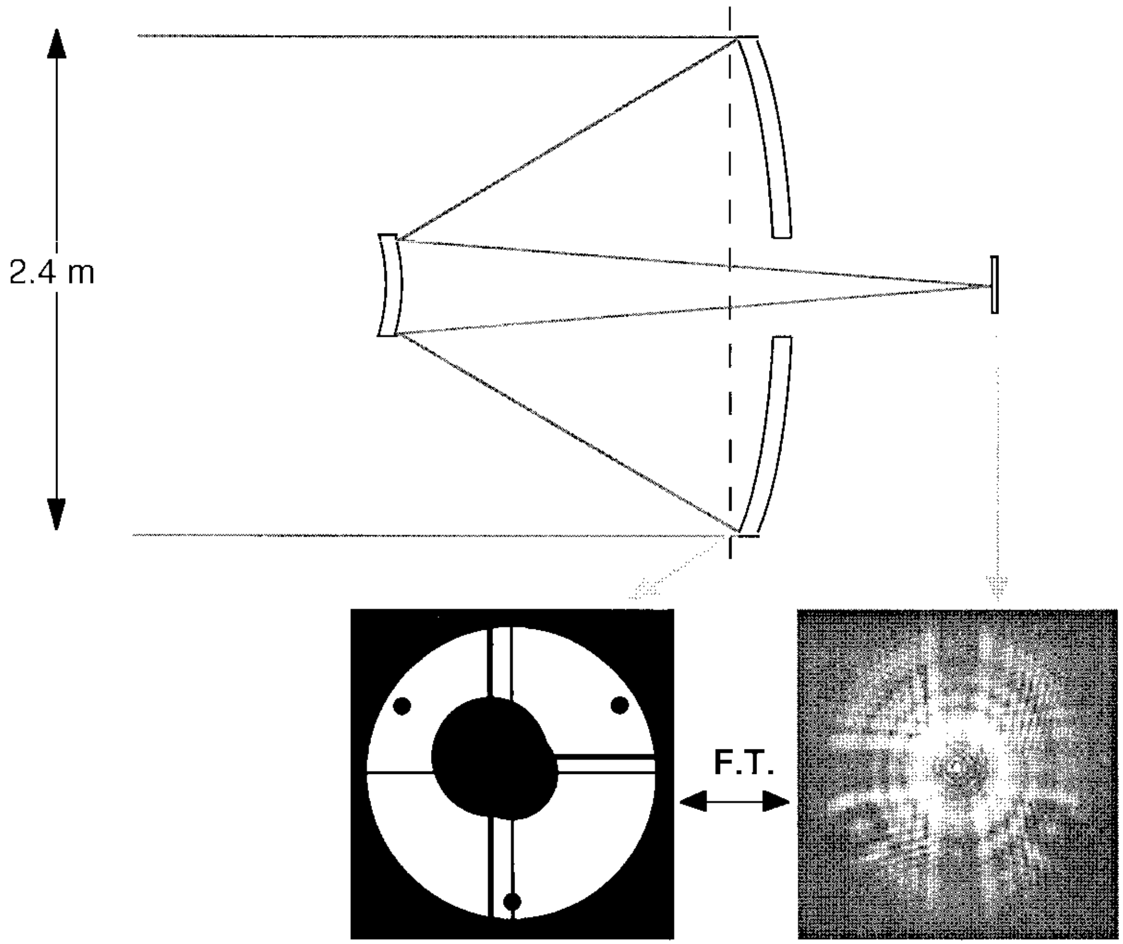

(Hubble Space Telescope)

Wavefronts in pupil plane and focal plane are related by a Fourier Transform

Techniques Employing Gradients

Minimize Error Metric, e.g.: $E = \sum_{u} W(u) \left[\, |G(u)| - |F(u)| \,\right]^2$

Contour Plot of Error Metric

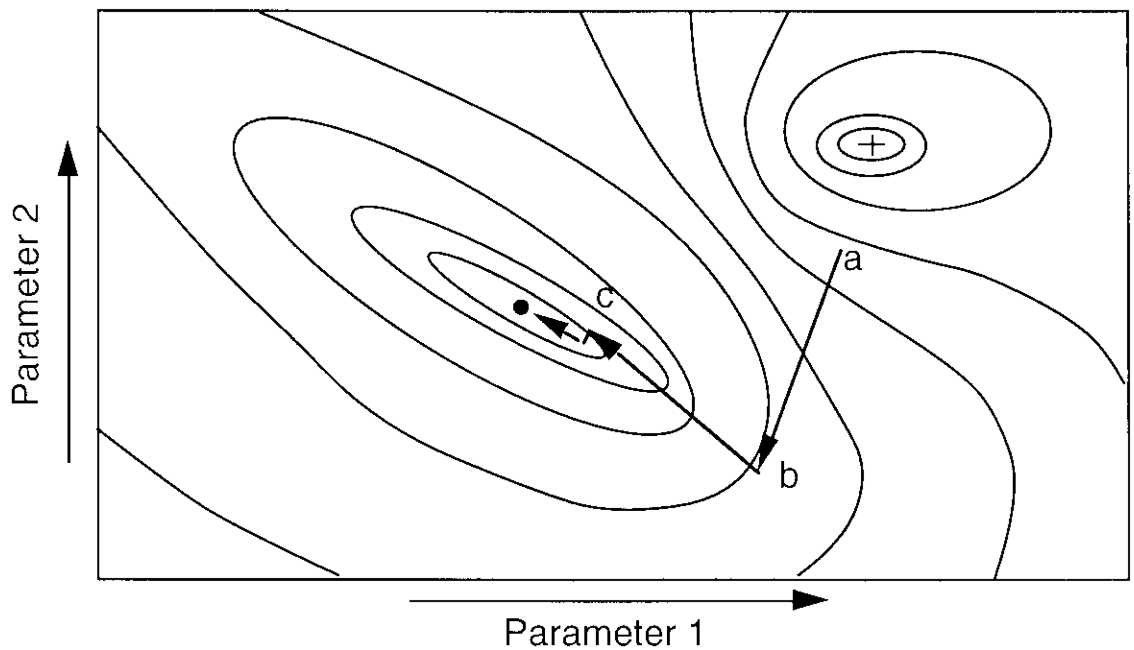

Repeat three steps:

1. Compute gradient: $\frac{\partial E}{\partial p_1}, \frac{\partial E}{\partial p_2}, \ldots$
2. Compute direction of search
3. Perform line search

Gradient methods: Steepest Descent
Conjugate Gradient
Davidon-Fletcher-Powell
...

Analytic Gradients

$$E = \sum_u W(u)\,[|G(u)| - |F(u)|]^2 \;,$$

For point-by-point phase map, $\theta(x)$,

$$\boxed{\frac{\partial E}{\partial \theta(x)} = 2\,\mathrm{Im}\{g(x)\,g^{w*}(x)\}}$$

For Zernike polynomial coefficients,

$$\boxed{\frac{\partial E}{\partial a_j} = 2\,\mathrm{Im}\left\{\sum_x g(x)\,g^{w*}(x)\,Z_j(x)\right\}} \;.$$

where

$$g(x) = m_o(x)\,e^{i\theta(x)} \;, \qquad \theta(x) = \sum_{j=1}^{J} a_j\,Z_j(x), \qquad G(u) = \mathcal{P}[g(x)] \;,$$

$$G^w(u) = W(u)\left[|F(u)|\,\frac{G(u)}{|G(u)|} - G(u)\right] \;, \text{ and } \qquad g^w(x) = \mathcal{P}^\dagger[G^w(u)] \;.$$

$\mathcal{P}[\bullet]$ can be a single FFT or multiple-plane Fresnel transforms with phase factors and obscurations

Analytic gradients very fast compared with calculation by finite differences

Hubble Telescope Retrieval Approach

- Pupil (support constraint) was known imperfectly
- Phase was relatively smooth and dominated by low-order Zernike's
  — Use boot-strapping approach

1. With initial guess for pupil, fit Zernike polynomial coefficients
   (parametric phase retrieval by gradient search)
2. With initial guess for Zernike polynomials, estimate pupil by ITA
   (retrieve magnitude, given an estimate of phase)
3. Redo steps 1 and 2 until convergence (2 iterations)
4. Estimate phase map by ITA, starting with Zernike polynomial phase
   (nonparametric phase retrieval by G-S or gradient search)
5. Refit Zernike coefficients to phase map
6. Redo steps 2 - 5

Phase Retrieval with Broadband, Undersampled Data:Background & Motivation

We wish to determine the aberrations of an optical system, given readily available information — measured point-spread functions (PSFs)

We can accomplish this using:

- Knowledge of the pupil function of the system,
- the Fourier reationship between the optical fields in the pupil and focal planes,
- and a phase retrieval algorithm

Previously used phase retrieval algorithms to determine wavefront aberrations:

— Analytic gradient search

— Iterative Transform (Gerchberg-Saxton) Algorithm

[1] J.R. Fienup, "Phase-Retrieval Algorithms for a Complicated Optical System," Appl. Opt. 32, 1737-1746 (1993).

[2] J.R. Fienup, J.C. Marron, T.J. Schulz and J.H. Seldin, "Hubble Space Telescope Characterized by Using Phase Retrieval Algorithms," Appl. Opt. 32 1747-1768 (1993).

Limitations of Previous Approaches

- Algorithm restrictions:
  - — Narrow-band light $\Delta\lambda/\lambda_c << 1$
    - – – Restricted retrieval to images through narrow-band filters only
  - — Nyquist-sampled data
    - – – Restricted retrieval to images from Hubble Space Telescope through filters with

      $\lambda_c > 0.500\ \mu m$ for Planetary Camera

      $\lambda_c > 1.667\ \mu m$ for Wide-Field Camera (none existed)
- Consequence: Could not use many of the available images of stars
- Solution: Generalized phase retrieval algorithm using physical model that includes wide-band light and undersampling

  + Computationally efficient analytic expression for gradient

Previous Wavefront Model, Error Metric, and Gradient

Wavefront in detector plane is Fourier transform of wavefront in pupil plane:

$$G(p,q) = P[g(m,n)] = \sum_{mn} g(m,n) \exp\left[-i2\pi\left(\frac{mp}{M} + \frac{nq}{N}\right)\right],$$

where $g(m,n) = A(m,n)\exp[i\phi(m,n)]$

where the phase error is given either by Zernike coefficients or point-by-point phase map: $\phi(m,n) = \sum_{j=1}^{J} a_j Z_j(m,n)$ or $\phi(m,n) = \phi_{pp}(m,n)$

To minimize Error Metric: $E = \sum_{p,q} W(p,q)\, [|G(p,q)| - |F(p,q)|]^2$

Use gradient (for example): $\dfrac{\partial E}{\partial a_j} = 2\,\mathrm{Im}\left\{\sum_{m,n} g(m,n)\, g^{W*}(m,n) Z_j(m,n)\right\}$

where $G^W(p,q) = W(p,q)G(p,q)\left[\dfrac{|F(p,q)|}{|G(p,q)|} - 1\right]$ and $g^W(m,n) = P^\dagger\left[G^W(p,q)\right]$

ERIM International, Inc.

Generalized Wavefront Model

Wavefront in detector plane is Fourier transform of wavefront in scaled pupil plane:

$$G_{\ell k}(p,q) = \left(\frac{\lambda_\ell}{\lambda_o}\right)\sum_{mn} A_\ell(m,n)\exp\left[i\frac{\lambda_o}{\lambda_\ell}\phi_{ok}\left(\frac{\lambda_o}{\lambda_\ell}m,\frac{\lambda_o}{\lambda_\ell}n\right)\right]\exp\left[-i2\pi\left(\frac{mp}{M}+\frac{nq}{N}\right)\right]$$

where the phase error has some Zernike coefficients that differ amongst images, others that are the same, and a point-by-point phase common to all:

$$\phi_{ok}(m,n) = \sum_{jd=2}^{4} a_{jd,k} Z_{jd}(m,n) + \sum_{js=5}^{J} a_{js} Z_{js}(m,n) + \phi_{opp}(m,n)$$

To avoid having to interpolate A and $\phi_{ok}(m,n)$ prior to FFT, perform interpolation during FFT by using:

$$G_{\ell k}(p,q) = \left(\frac{\lambda_o}{\lambda_\ell}\right)\sum_{mn} A_o(m,n)\exp\left[i\frac{\lambda_o}{\lambda_\ell}\phi_{ok}(m,n)\right]\exp\left[-i2\pi\left(\frac{mp}{M_\ell}+\frac{nq}{N_\ell}\right)\right]$$

where $M_\ell = \dfrac{\Delta u \Delta x}{\lambda_\ell z_f} = M_o\dfrac{\lambda_o}{\lambda_\ell}$, and λ_o is a reference wavelength

(pick λ_ℓ's so that M_ℓ's are highly composite numbers for efficient FFT's)

Generalized Error Metric

Minimize a weighted, normalized, mean-squared error metric:

$$E = K^{-1}\sum_{k=1}^{K}\Phi_k^{-1}\sum_{pq}W_k(p,q)grid(p,q)\left[\alpha_k\sqrt{\sum_{\ell=1}^{L}S_\ell\left|G_{\ell k}(p,q)\right|^2 * D(p,q)} - |F|_k(p,q)\right]^2$$

where S_ℓ = Spectral response at ℓ^{th} wavelength, λ_ℓ,

$* D(p,q)$ = convolution with detector pixel area,

α_k = normalization factor to give computed k^{th} psf the same strength as $|F|_k$

$|F|_k$ = the square root of the k^{th} measured, corrected data,

$grid(p,q)$ = the pixel sampling function

$W_k(p,q)$ = a pixel-by-pixel weighting function for k^{th} data set

$\Phi_k = \Phi_k = \sum_{pq}W_k(p,q)\left[|F|_k(p,q)\right]^2$ is the weighted energy in the k^{th} data set

Efficient Analytic Gradients

Have derived analytic gradients for partial derivatives of E with respect to
$a_{jd,k}$ = Zernike coefficients that differ amongst data sets, a_{js} = Zernike coef.s same for all data sets,
$\phi_{opp}(m, n)$ = Point-by-point phase map, $A_o(m, n)$ = Point-by-point aperture function
α_k = PSF weighting function

allowing various combinations of terms to be held fixed or optimized.

For example for pixel-by-pixel phase,

$$\frac{\partial E}{\partial \phi_{pp}(m_1, n_1)} = \frac{-2}{K} \sum_{k=1}^{K} \frac{\alpha_k^2}{\Phi_k} \sum_{\ell=1}^{L} S_\ell \left(\frac{\lambda_o}{\lambda_\ell} \right)^2 \operatorname{Im}\left[g_\ell(m_1, n_1) g_{\ell k}^{W*}(m_1, n_1) \right],$$

where $g_\ell(m_1, n_1)$ is the field in the aperture, and

$$g_{\ell k}^{W*}(m_1, n_1) = \sum_{p_1 q_1} \exp\left[-i2\pi \left(\frac{m_1 p_1}{M_\ell} + \frac{n_1 q_1}{N_\ell} \right) \right] G_{\ell k}^*(p_1, q_1) \times \sum_{pq} D(p - p_1, q - q_1) W_k(p, q) grid(p, q) \left[1 - \frac{F_k(p, q)}{\alpha_k \sqrt{\sum_{\ell=1}^{L} S_\ell \left| G_{\ell k}(p, q) \right|^2 * D(p, q)}} \right]$$

This requires $2LK$ FFT's

Minimize Error metric using gradient-based nonlinear optimization code

Used Matlab's *fminu* with options:
Broyden/Fletcher/Goldfarb/Shanno or Davidon/Fletcher-Powell quasi-Newton
and for point-by-point phase functions or aperture amplitudes:Conjugate Gradient (no Hessian required)
all using a mixed quadratic and cubic line search

Simulated Star Images

(a) polychromatic PSF a

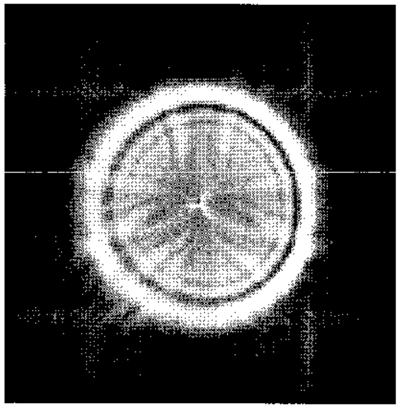

(b) polychromatic PSF b

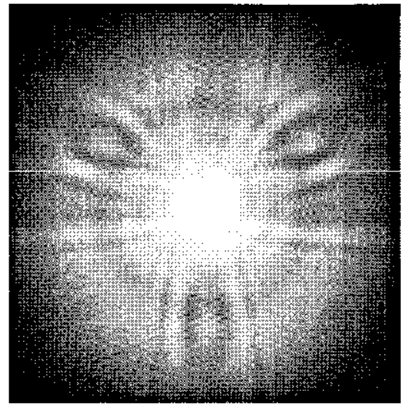

(c) monochromatic PSF a

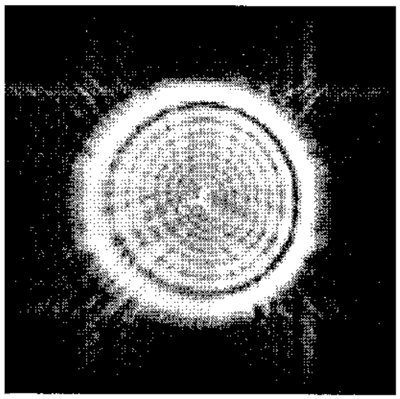

(d) monochromatic PSF b

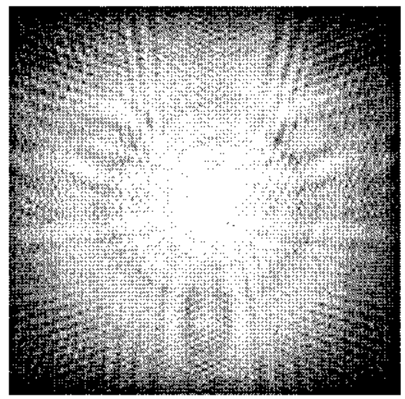

- –0.30 μm rms Spherical, small amounts of others; • 2x2 pixel integration;
- WF/PC F555W filter, $\{\lambda_i\} = \{472.5, 516.0, 562.5, 609.0, 656.0\}$ nm

$$\{S_i\} = \{\ 0.78,\ \ 0.91,\ \ 0.82,\ \ 0.50,\ \ 0.18\}$$

Error Metric Versus Iteration Number

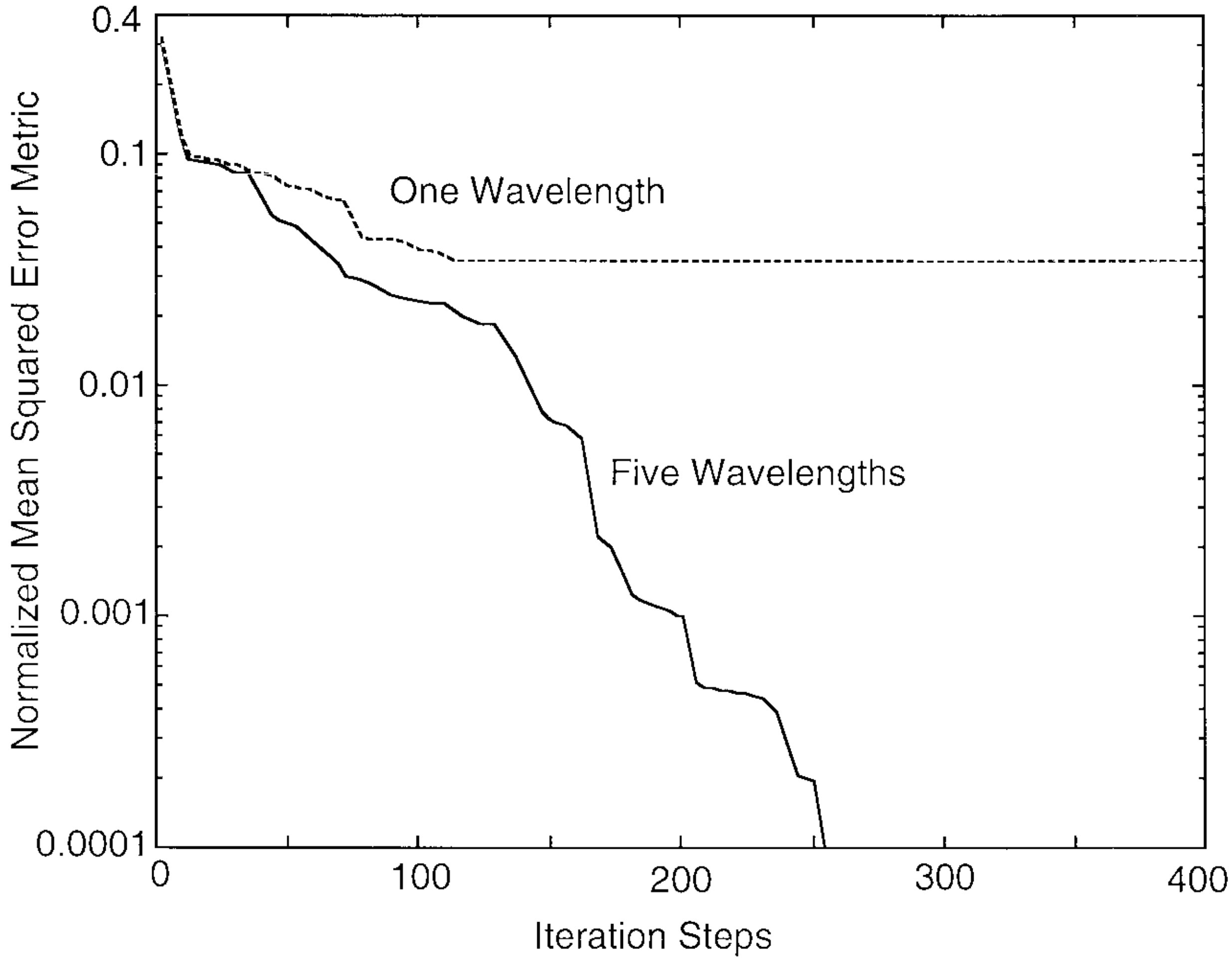

One iteration step = one function evaluation

(typically 3 to 6 function evaluations per gradient caculation)

Pupil-Plane Imaging

Problem:

$\rho = \lambda R/D$: For fine resolution, need short wavelength and large aperture
– Large apertures are heavy and expensive

Also, atmospherics and imperfect optics cause aberrations & blur images

Solution:

Laser illumination — Ensures adequate light level; Day/night operation
— Enables unconventional coherent imaging modalities

Pupil-plane sensing — Minimum depth ==> light weight, low cost

Sparse, distributed detector array
— Further reduce weight and cost

Phase retrieval & array phasing algorithms
needed to correct phase errors

- **Trades more computer processing for less complicated optical hardware**

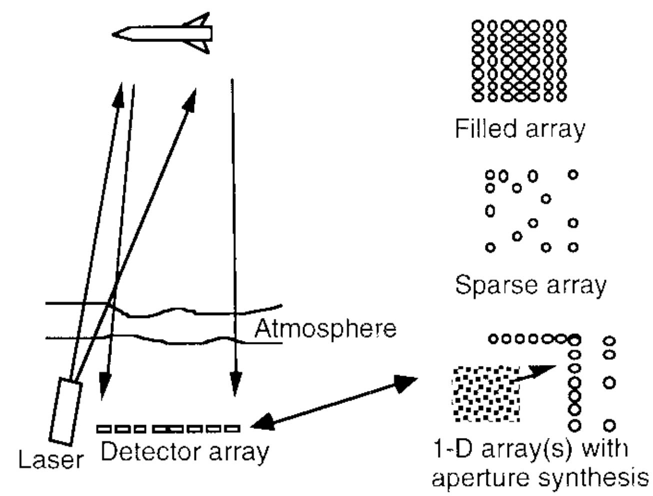

Reconstruction of Complex-Valued Images

- No nonnegativity constraint, so use only support constraint
- Support constraint must be good
  - Asymmetric (e.g., triangle, not rectangle or ellipse)
  - Nonconvex
  - Tight

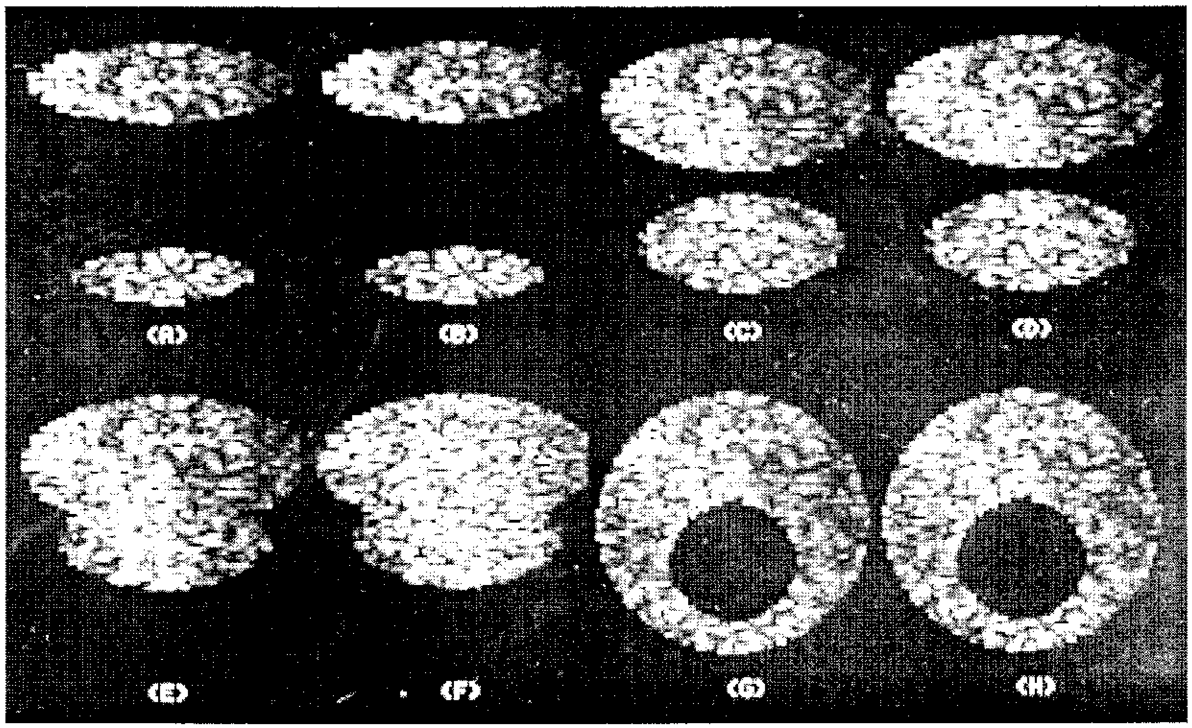

Complex-Valued Image Reconstruction Using Phase over Part of Aperture

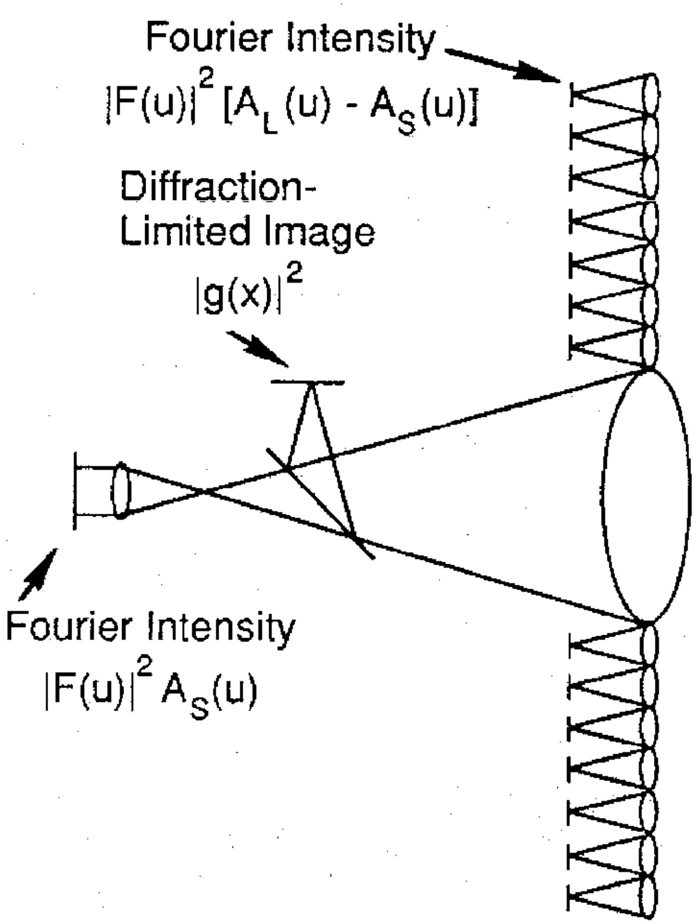

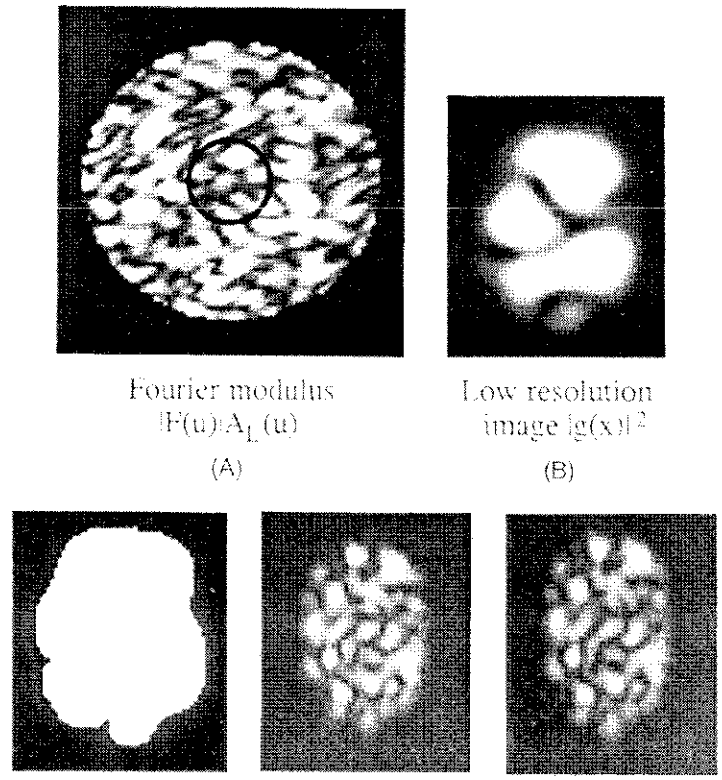

Fourier modulus $|F(u)|A_L(u)$ (A)

Low resolution image $|g(x)|^2$ (B)

Support constraint $S(x)$ (C)

Reconstructed image $\hat{f}(x)$ (D)

Ideal image $f(x)$ (E)

- J.R. Fienup and A.M. Kowalczyk, "Phase Retrieval for a Complex-Valued Object by Using a Low-Resolution Image," J. Opt. Soc. Am. A 7, 450-458 (1990).

VERIDIAN
Systems Division

Convergence of Complex-Valued Image Reconstruction Using Phase over Part of Aperture

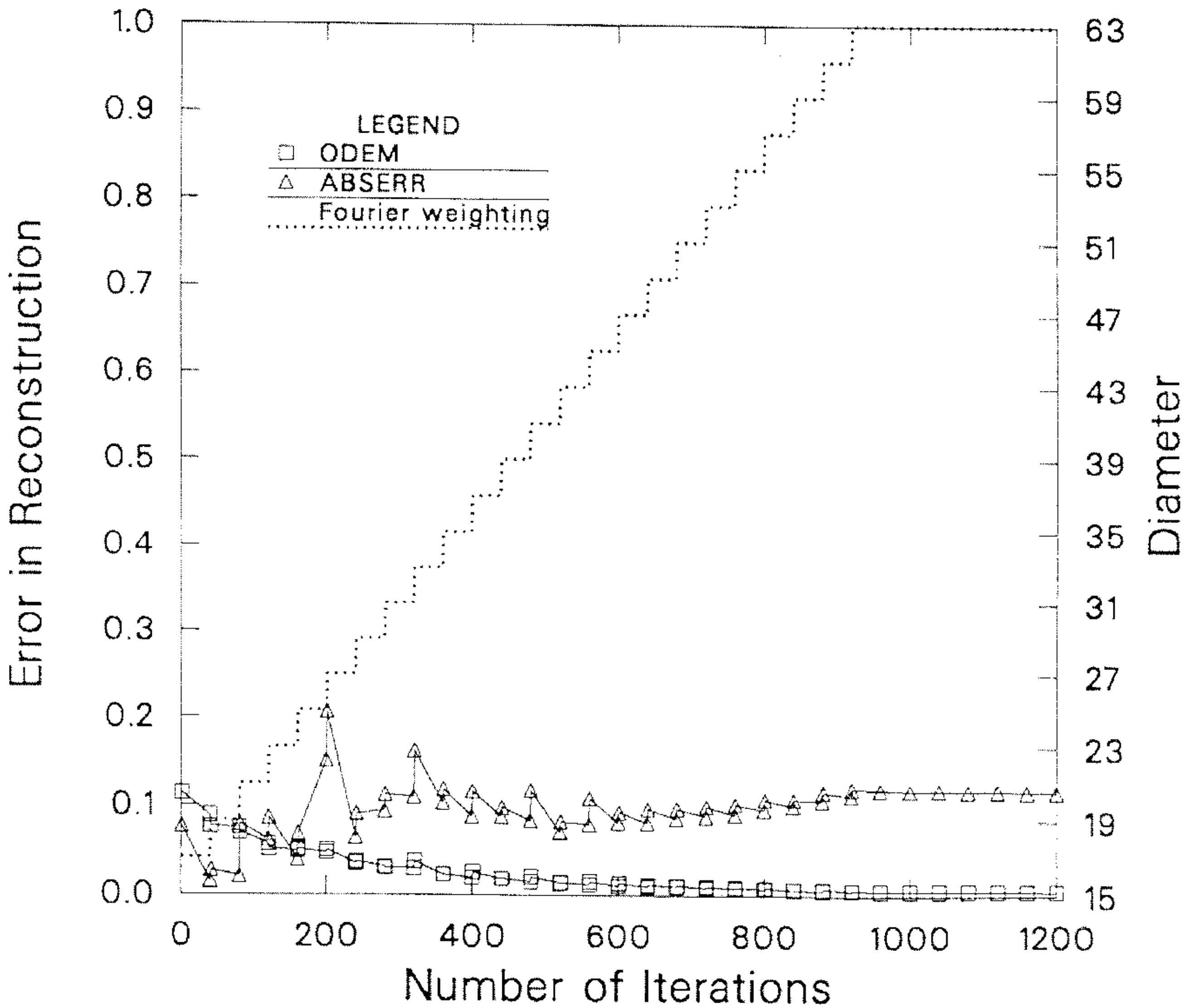

JPF 5/01

VERIDIAN
ERIM International

PROCLAIM 3-D Imaging Concept

Phase Retrieval with Opacity Constraint LAser IMaging

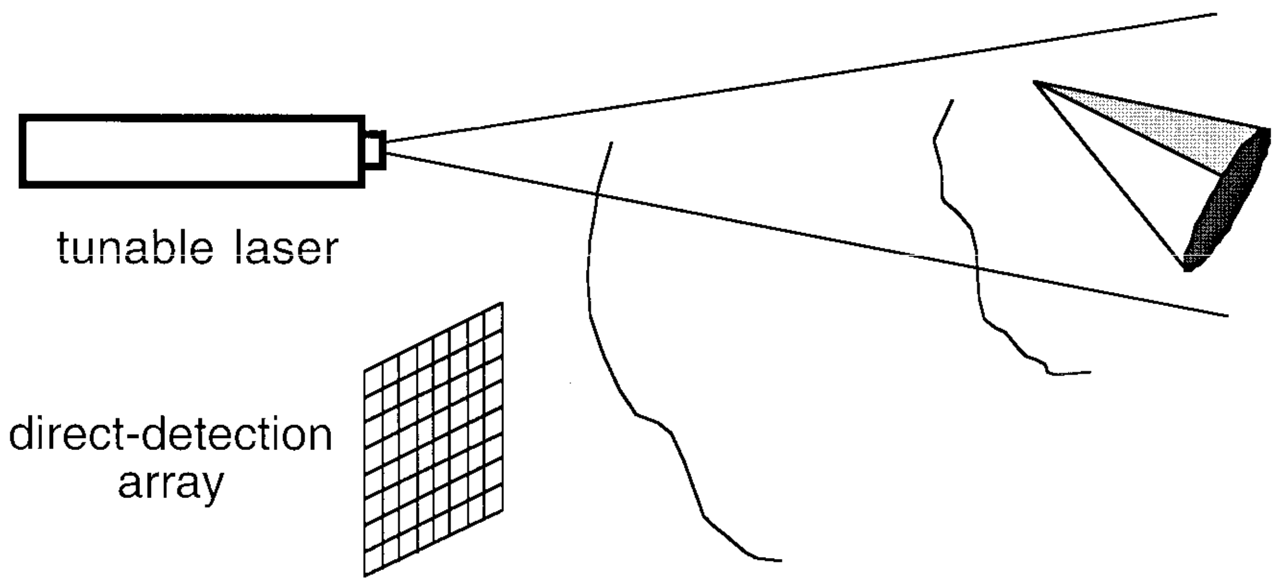

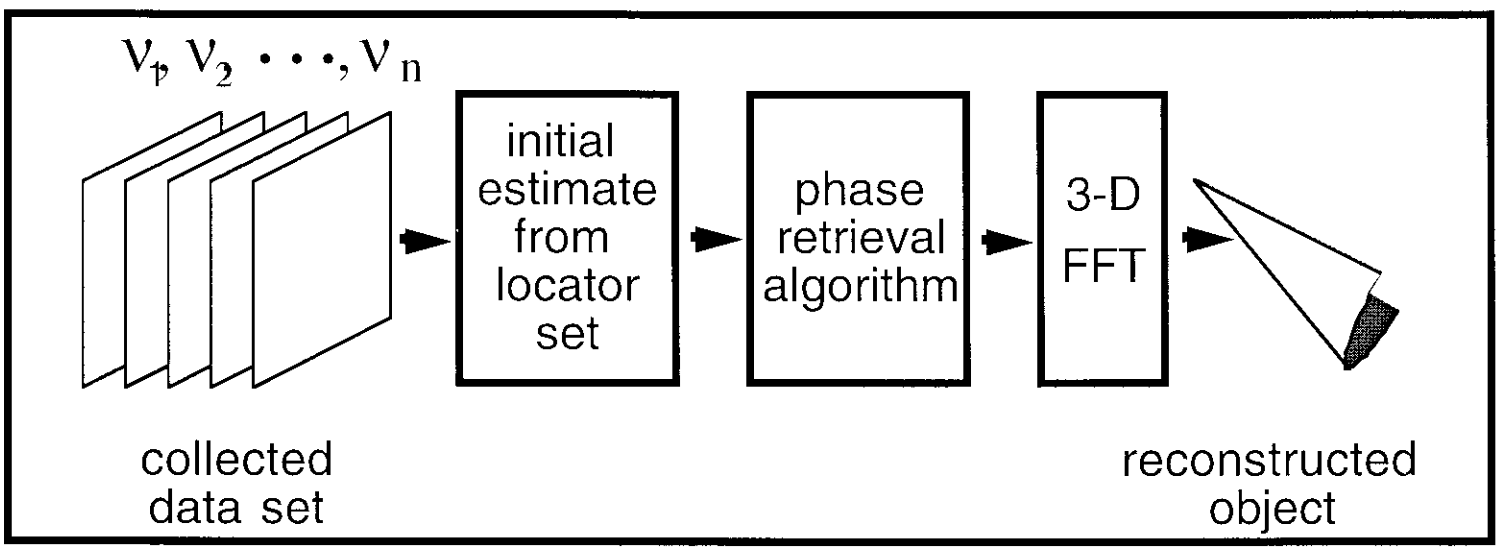

Imaging Correlography

- Get incoherent-image information from coherent speckle pattern

Incoherent Fourier squared magnitude:

$$|F_I(u, v, w)|^2 \approx \langle [D_k(u, v, w) - I_o] \star [D_k(u, v, w) - I_o] \rangle_k$$

Incoherent object autocorrelation:

$$r_{fI}(x, y, z) \approx \langle |r_k(x, y, z)|^2 \rangle_k - b\,|a(x, y, z)|^2$$

where $r_k(x, y, z) = \mathcal{F}[D_k(u, v, w)]$ is coherent autocorrelation of image

- Easier phase retrieval since have nonnegativity constraint on incoherent image
- Coarser resolution since correlography SNR lower

Data Processing Steps for PROCLAIM with Correlography

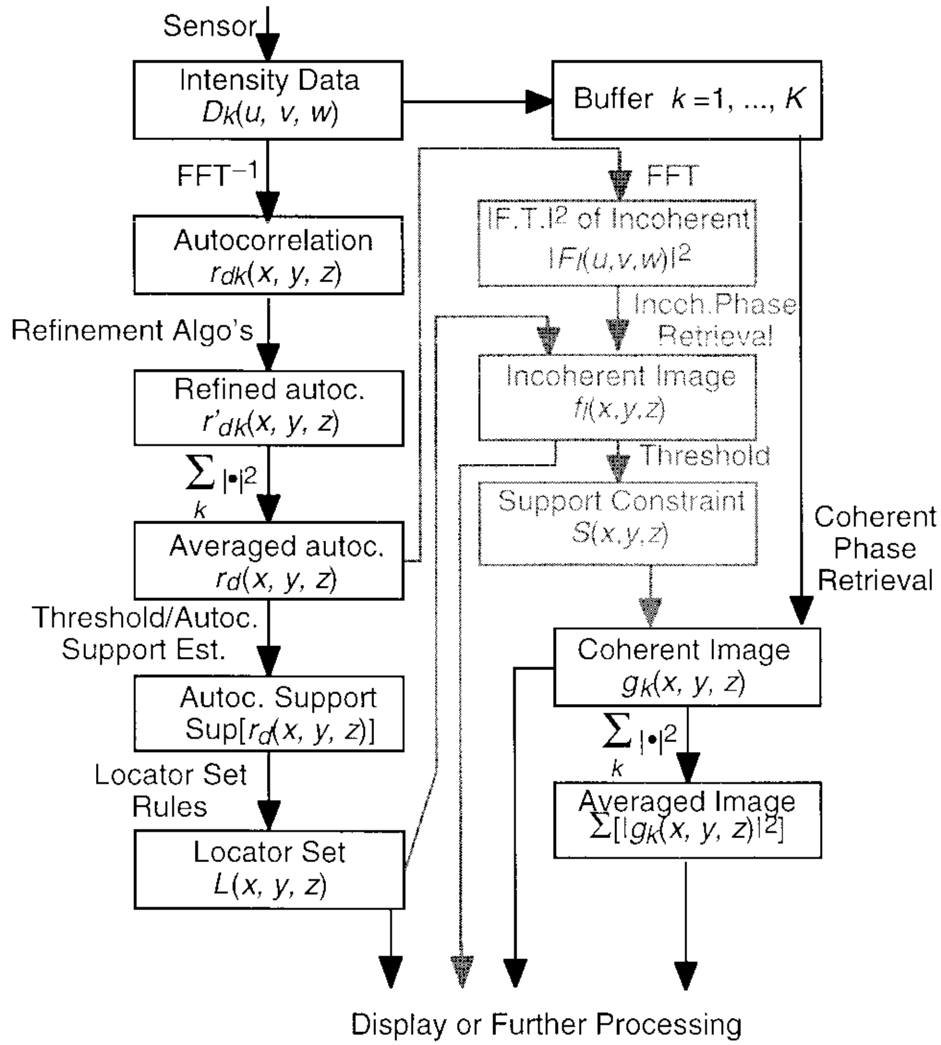

Object for Laboratory Experiments

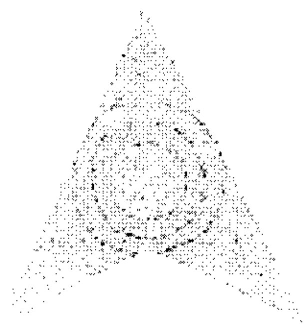

ST Object. The three concentric discs forming a pyramid can be seen as dark circles at their edges. The small piece on one of the two lower legs was removed before this photograph was taken.

VERIDIAN
ERIM International

Collected Fourier Intensity Data

Data cube:

1024x1024 CCD pixels
x 64 wavelengths

Shown at right:
128x128x64 sub-cube

(128x128 CCD pixels at each of 64 wavelengths)

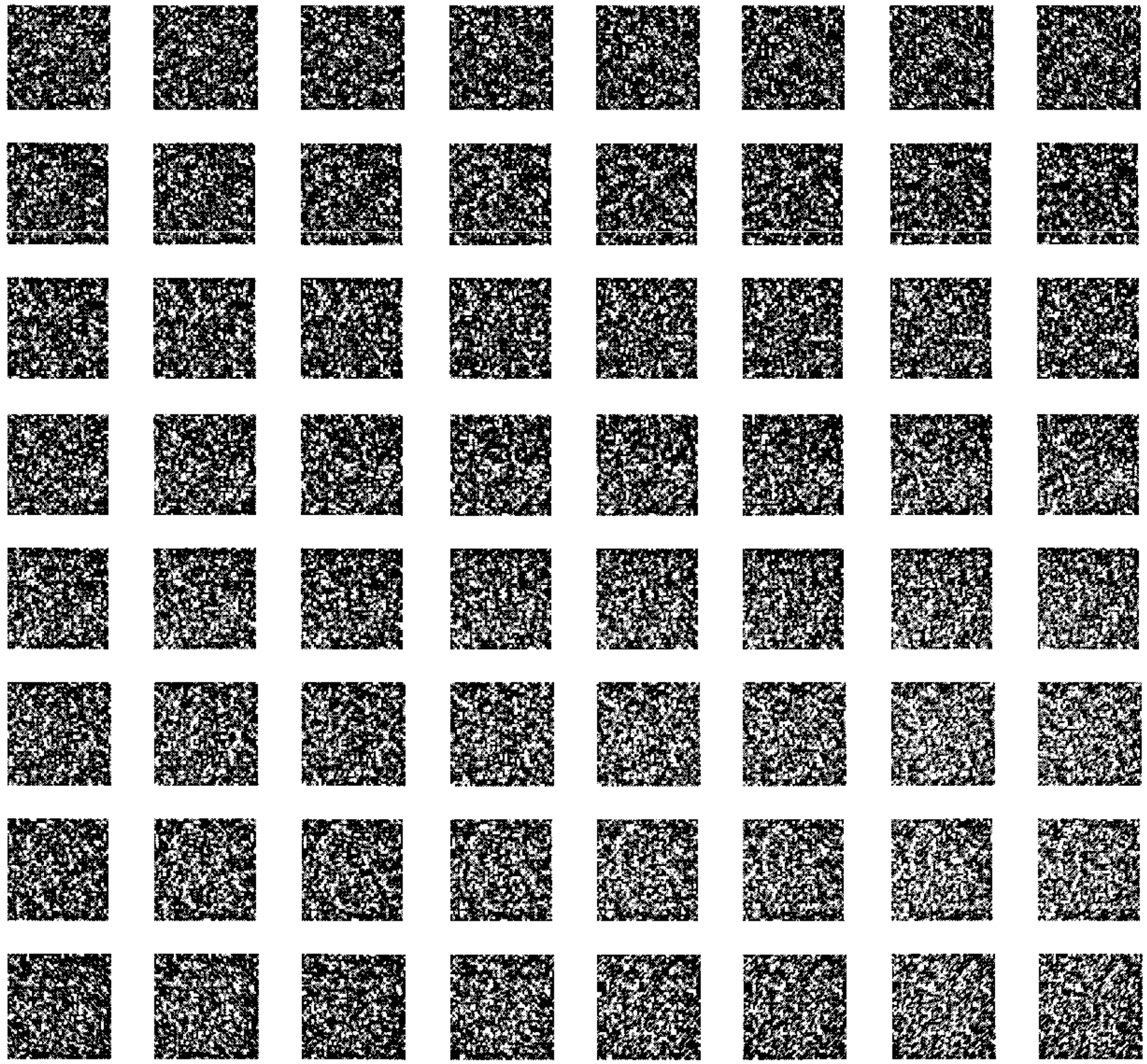

VERIDIAN
ERIM International

3-D Image Reconstructed by ITA from Laboratory-Collected PROCLAIM Data

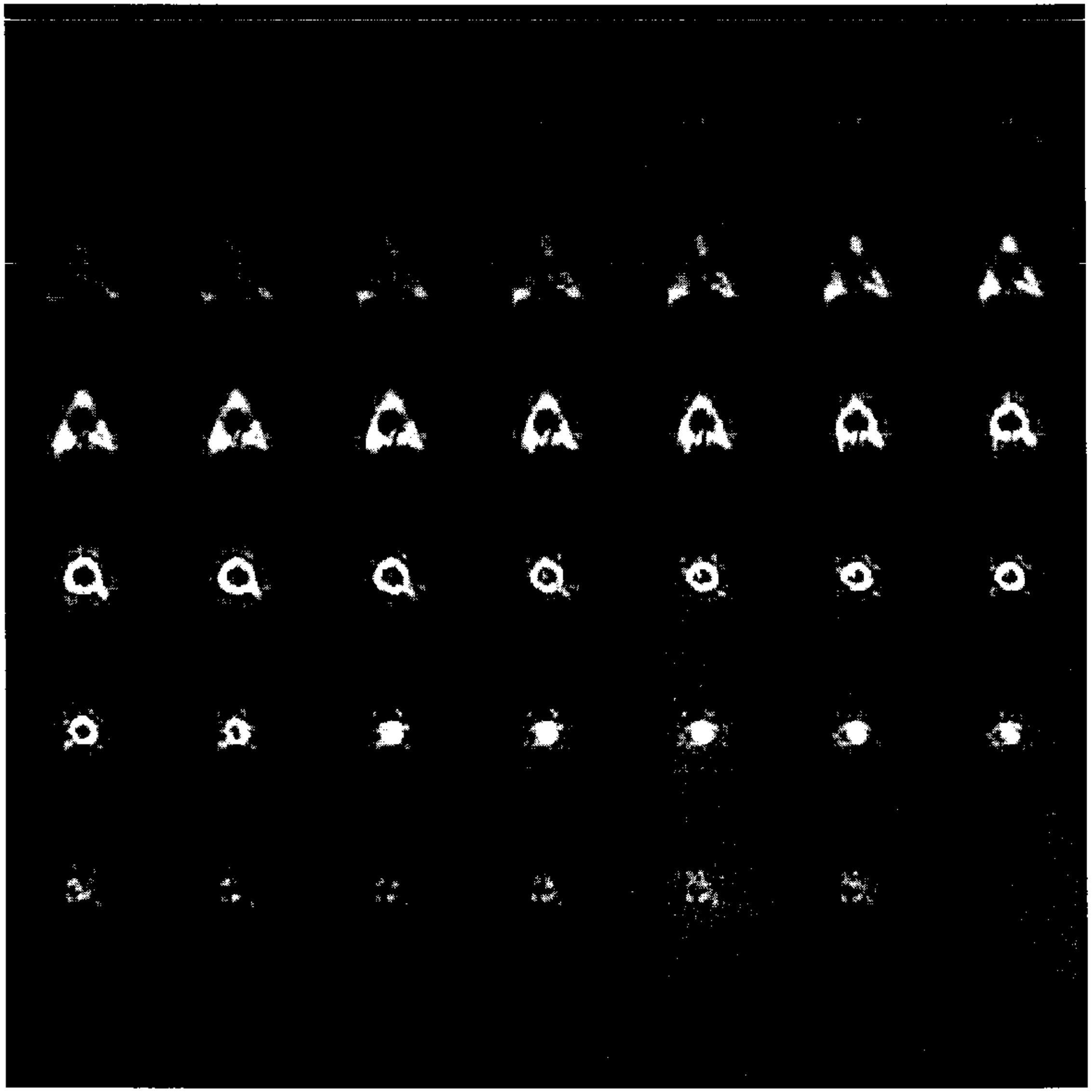

(x-y slices at a succession of planes at different depths)

Close Cousin to Phase Retrieval: SAR Autofocus

Signal (phase) history = Fourier transform of image

Measure $G(x, v) = F(x, v) \exp[i\phi_e(v)]$

F = ideal signal history

ϕ_e = phase error = $4\pi\, \Delta r/\lambda$

x = range, v = slow time

Δr = unknown radial motion

SAR platform motion

Ionospheric phase error

Target motion (ISAR)

Problem, given signal history $G(x, v)$,

what *a priori* information can we employ to determine $\phi_e(v)$?

Image Sharpening Algorithm

- For an initial phase estimate, compute corrected image $G(x,v) = G_d(x,v)\exp[-i\phi(v)]$

$$g(x,y) = FT^{-1}[G(x,v)]$$

- Find $\phi(v)$ that maximizes the sharpness of the image:

$$S_1 = \sum_{x,y} |g(x,y)|^4 = \sum_{x,y} \left[|g(x,y)|^2\right]^2 = \sum_{x,y} [I(x,y)]^2 \qquad S_\Gamma = \sum_{x,y} \Gamma\left[I(x,y)\right]$$

- Efficient algorithm = Conjugate gradient search over $\phi(v)$ using analytic gradient:

$$\frac{\partial S_\Gamma}{\partial \phi(v)} = 2(1/N)\sum_x w(x)\,\mathrm{Im}\left\{ G(x,v)\left(FT\left[g(x,y)\frac{\partial \Gamma[I(x,y)]}{\partial I(x,y)} \right]\right)^* \right\}$$

- Can also optimize over coefficients of polynomial expansion of phase:

$$\phi(v) = \sum_{j=1}^{J} a_j L_j(v) \qquad \frac{\partial S_\Gamma}{\partial a_j} = (2/N)\sum_v L_j(v)\sum_x w(x)\,\mathrm{Im}\left\{ G(x,v)\left(FT\left[g(x,y)\frac{\partial \Gamma[I(x,y)]}{\partial I(x,y)} \right]\right)^* \right\}$$

- Use standard gradient search algorithms
  e.g., conjugate gradient

VERIDIAN

ERIM International

SAR Focusing Example: Maximizing Sharpness

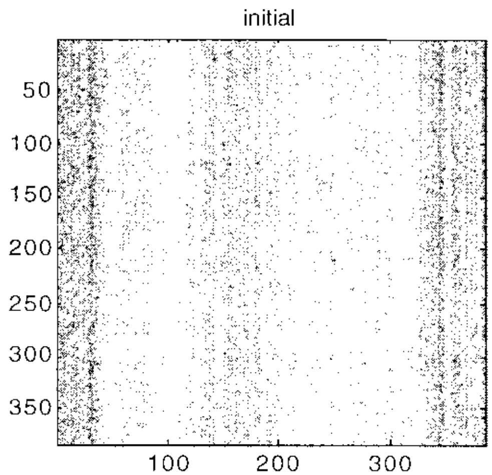

Initial Blurred Image (0 Iterations)

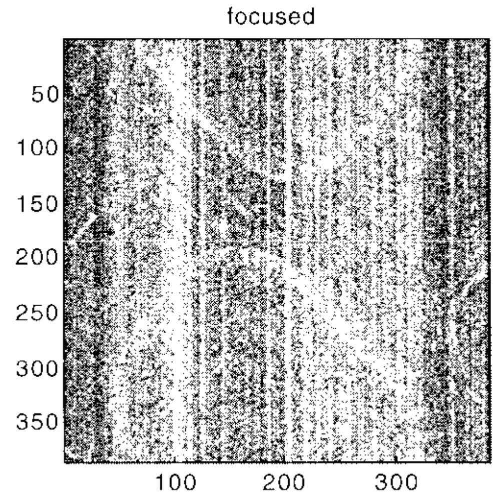

Focused after 50 Iterations

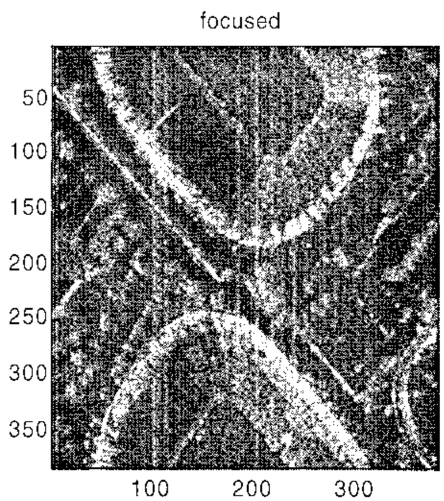

Focused after 100 Iterations

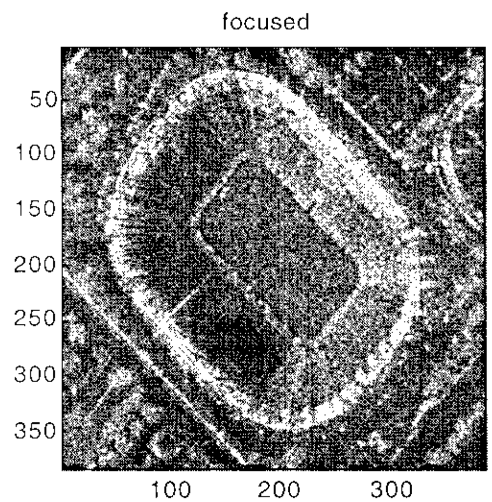

Focused after 200 Iterations
(and recentered)

VERIDIAN Systems Division

References Than Influenced Me The Most

- N.C. Gallagher and B. Liu, "Method for Computing Kinoforms that Reduces Image Reconstruction Error," Appl. Opt. 12, 2328-2335 (1973).
- R.W. Gerchberg and W.O. Saxton, "A Practical Algorithm for the Determination of Phase from Image and Diffraction Plane Pictures," Optik 35, 237-246 (1972).
- R.W. Gerchberg, "Super-Resolution through Error Energy Reduction," Optica Acta 21, 709-720 (1974).
- W.O. Saxton, Computer Techniques for Image Processing in Electron Microscopy (Academic Press, New York, 1978).
- D.C. Youla, "Generalized Image Restoration by Method of Alternating Orthogonal Projections," IEEE Trans. Circuits and Systems CAS-25, 694-702 (1978).
- Yu.M. Bruck and L.G. Sodin, "On the Ambiguity of the Image Reconstruction Problem," Opt. Commun. 30, 304-308 (1979).
- R.A. Gonsalves, "Imaging with Phase Diversity," ICO-12 Meeting, Graz, Austria, September 1981.


MICHIGAN
PHASE R
150